

A Phenomenological Acceleration Law from Galaxy Dynamics Consistent with Type Ia Supernova Distances

Donald Airey,^{1*}

¹*Worcester Polytechnic Institute, 100 Institution Road, Worcester, MA 01609, USA*

Accepted XXX. Received YYY; in original form ZZZ

ABSTRACT

We test whether a single empirically determined acceleration scale can link galaxy dynamics and cosmological distance measurements. A phenomenological acceleration law is fit directly to galaxy kinematic data from the SPARC sample, yielding a fixed acceleration scale and reproducing the baryonic Tully–Fisher relation as a derived consequence. This scale defines an analytic, closed-form distance–redshift relation, which is evaluated against the Pantheon+SH0ES Type Ia supernova dataset in a predictive setting.

The resulting relation predicts Type Ia supernova distances with a significantly lower covariance-weighted χ^2 than a spatially flat FLRW model with Planck 2018 parameters under identical, out-of-sample evaluation conditions, providing a compact and computationally efficient representation of the observed distance–redshift relation in this empirical test.

Key words: cosmology: observations – distance scale – supernovae: general – galaxies: kinematics and dynamics

1 INTRODUCTION

Type Ia supernovae (SNe Ia) provide one of the most direct observational probes of the cosmic expansion history through the luminosity distance–redshift relation. Large compilations such as Pantheon+ Brout et al. (2022), building on earlier compilations Scolnic et al. (2018), and constructed using standard light-curve fitting techniques such as SALT2 Guy et al. (2007), enable high-precision tests of cosmological models using covariance-weighted statistical methods. In the standard framework, Type Ia supernova observations are interpreted within a parameterized expansion history specified by the Hubble constant and the relative contributions of matter, radiation, and dark energy, with spatial flatness often assumed. These parameters determine the redshift dependence of the expansion rate $H(z)$ and, through it, the luminosity distance.

An alternative approach is to consider constrained analytic forms for the distance–redshift relation and to evaluate their performance directly against the data. In this work, we examine a model in which the distance relation is parameterized by a small set of kinematic quantities, one of which is an acceleration scale determined independently from galaxy dynamics. This approach enables a direct test of whether a single empirically determined scale can consistently describe both galactic and cosmological observables.

The acceleration scale is obtained by fitting the phenomenological acceleration law directly to galaxy kinematic data from the SPARC sample, yielding a fixed value that is not adjusted in the supernova analysis. The remaining parameter is calibrated using the Cepheid subset of the Pantheon+ sample, and the resulting model is evaluated on the out-of-sample supernovae using the full covariance matrix.

The goal of this paper is to assess whether this constrained ana-

lytic relation provides a quantitatively consistent description of the observed SNe Ia distance moduli across redshift under identical calibration conditions. No assumption is made regarding the underlying gravitational or cosmological theory, and the analysis is restricted to the observables considered here.

2 PHENOMENOLOGICAL ACCELERATION LAW

The purpose of this work is to test whether a single empirically determined acceleration scale can link two otherwise distinct observational regimes: circular motion in rotationally supported galaxies and the luminosity distances of Type Ia supernovae. We define a phenomenological acceleration law for circular orbits, determine the acceleration scale A from the baryonic Tully–Fisher relation, and then hold it fixed in the supernova analysis. No underlying gravitational theory is assumed. This separation is essential: the acceleration scale entering the distance–redshift relation is not fitted to the supernova sample.

2.1 Circular Orbits

We consider circular motion in an acceleration field consisting of a Newtonian component and a constant inward term A . For a test body in a circular orbit of radius r about an enclosed baryonic mass $M_b(r)$, the radial acceleration is

$$a(r) = -A - \frac{GM_b(r)}{r^2}. \quad (1)$$

The condition for circular motion requires that this radial acceleration provide the centripetal acceleration,

$$-\frac{v^2}{r} = -A - \frac{GM_b(r)}{r^2}. \quad (2)$$

* E-mail: don@airey.us

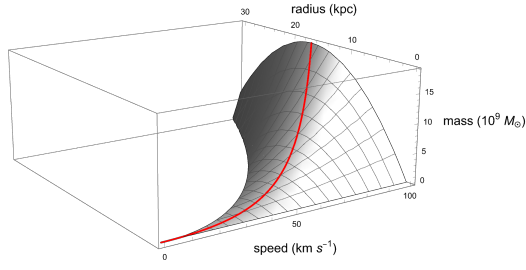


Figure 1. Circular-orbit solution surface defined by equation (4). The baryonic mass surface $M(v, r)$ is shown as a function of orbital speed v and orbital radius r for an illustrative acceleration scale $A = 10^{-11} \text{ m s}^{-2}$. The red ridge marks the locus $M_{\text{max}}(v)$ corresponding to the maximum baryonic mass permitted at each orbital speed. Galaxies populating this ridge reproduce the baryonic Tully–Fisher relation.

Multiplying by r gives

$$v^2 = Ar + \frac{GM_b(r)}{r}, \quad (3)$$

and solving for the enclosed baryonic mass yields

$$M_b(r) = \frac{r(v^2 - Ar)}{G}. \quad (4)$$

2.2 Circular-Orbit Solutions

Equation (4) defines a two-parameter family of circular-orbit solutions relating baryonic mass M , orbital radius r , and orbital speed v .

For fixed orbital speed v , the mass function $M(r)$ is a concave quadratic in r . Differentiating gives

$$\frac{dM}{dr} = \frac{v^2 - 2Ar}{G}. \quad (5)$$

The mass therefore reaches a maximum at

$$r_{\text{max}} = \frac{v^2}{2A}. \quad (6)$$

Substituting this radius into equation (4) yields the maximum baryonic mass compatible with a circular orbit at speed v ,

$$M_{\text{max}}(v) = \frac{v^4}{4AG}. \quad (7)$$

The surface $M(v, r)$ defines a family of circular-orbit solutions, as shown in Figure 1, with the ridge $M_{\text{max}}(v)$ giving the upper envelope of baryonic mass for a given orbital speed. Galaxies dominated by circular rotation are expected to saturate this boundary and follow a characteristic mass–velocity relation.

2.3 Baryonic Tully–Fisher Relation

$M_{\text{max}}(v)$ defines the scaling $M \propto v^4$, consistent with the observed baryonic Tully–Fisher relation in [McGaugh et al. \(2000\)](#). The normalization of this relation is set by the acceleration scale A . A characteristic acceleration scale in galaxy dynamics has previously been emphasized in frameworks such as MOND [Milgrom \(1983\)](#).

This parameter is determined empirically by fitting the circular-orbit envelope (equation (7)) to the SPARC galaxy sample of [McGaugh, Lelli and Schombert \(2016\)](#), using the assumptions $Y_{\star} = 0.5$, $f_{\text{gas}} = 1.33$, zero intrinsic mass-to-light uncertainty, and the quality cut $\text{Qual} \leq 3$. These rotationally supported disk

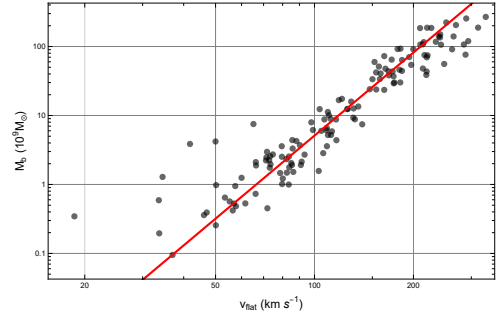


Figure 2. Log–log plot of baryonic mass M_b versus outer rotation speed v for the SPARC galaxy sample. Black circles show the observed galaxies. The solid red line shows the circular-orbit envelope evaluated at the best-fit acceleration, demonstrating consistency with the observed $M \propto v^4$ scaling.

systems are well suited to this analysis, as their kinematics closely follow circular-orbit behavior.

For each galaxy the rotation curve provides an asymptotic circular velocity v , while the baryonic mass M_b is computed as $M_b = Y_{\star}L_{3.6} + f_{\text{gas}}M_{\text{HI}}$. The value of A is determined by minimizing the χ^2 statistic between the theoretical envelope and the observed (M_b, v) pairs.

The best-fit acceleration scale is

$$A = 3.7 \times 10^{-11} \text{ m s}^{-2}. \quad (8)$$

The observed galaxies follow the predicted $M \propto v^4$ scaling, as shown in Figure 2. In this construction, the baryonic Tully–Fisher relation is not imposed but follows directly from the acceleration law, with the constant acceleration scale setting its normalization.

2.4 Distance–Redshift Relation

With the acceleration scale fixed empirically from galaxy dynamics, we now construct a phenomenological analytic form for the comoving distance,

$$D_C(z) = \frac{t_o(2V_0 - At_o)z}{2+z}, \quad (9)$$

where t_o and V_0 set the temporal and velocity scales of the relation, respectively. The luminosity distance follows as

$$D_L(z) = (1+z)D_C(z). \quad (10)$$

This closed-form expression differs from the standard FLRW integral representation and provides an alternative distance–redshift relation for direct comparison with observations.

2.5 Distance Modulus

Type Ia supernova observations are reported in terms of the distance modulus [Tripp \(1998\)](#), which relates the observed luminosity distance to the measured brightness of each supernova,

$$\mu(z) = 5 \log_{10} \left(\frac{D_L(z)}{10 \text{ pc}} \right). \quad (11)$$

2.6 Kinematic Parameters

We treat the parameters in the analytic distance–redshift relation as kinematic quantities that set the temporal, velocity, and acceleration scales of the model, without assuming an underlying dynamical theory.

Parameter	Value
A	$3.7 \times 10^{-11} \text{ m s}^{-2}$
V_0	$3.16 \times 10^8 \text{ m s}^{-1}$
t_o	$4.51 \times 10^{17} \text{ s}$

Table 1. Kinematic parameters determined from galaxy kinematics and the Cepheid-calibrated Pantheon+ subset.

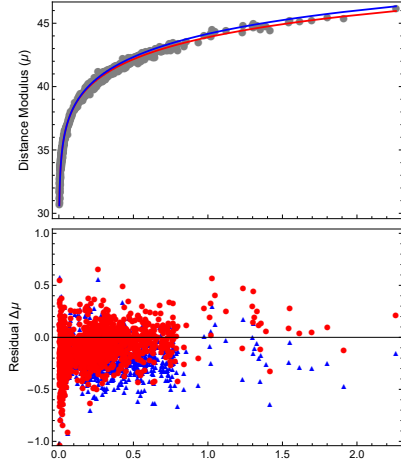


Figure 3. Pantheon+SH0ES distance moduli as a function of redshift z , compared with the analytic model prediction and the spatially flat FLRW model. Model parameters are fixed by BTFR and Cepheid calibrations, and the comparison is shown for the remaining supernovae. FLRW parameters are fixed to the Planck 2018 values. Residuals are shown for the analytic model (red circles) and FLRW (blue triangles).

A boundary condition is imposed at the observation time t_o by requiring that the parameter combination reproduce the locally measured speed of light,

$$c = V_0 - At_o. \quad (12)$$

This condition fixes the integration constant V_0 in the analytic distance relation. Rearranging,

$$V_0 = c + At_o. \quad (13)$$

With the acceleration scale A fixed from the galaxy kinematic analysis, the Cepheid subset Riess et al. (2022) is used to determine the temporal scale t_o , leaving a single free parameter. For each candidate value of t_o , theoretical distance moduli $\mu_{\text{th}}(z)$ are evaluated and compared with the observed values $\mu_{\text{obs}}(z)$, defining residuals

$$r_i = \mu_{\text{obs}}(z_i) - \mu_{\text{th}}(z_i). \quad (14)$$

The best-fit value of t_o is obtained by minimizing the covariance-weighted statistic

$$\chi^2 = r^T C^{-1} r, \quad (15)$$

where C is the full Pantheon+ STAT+SYS covariance matrix. The resulting value of t_o determines V_0 , completing the kinematic parameter set. The fitted parameters are listed in Table 1.

2.7 Type Ia Supernovae

We compare the analytic distance–redshift relation with the Pantheon+SH0ES Type Ia supernova dataset using covariance-weighted

Model	χ^2	ν	χ^2/ν
Analytic model	2726	1625	1.68
FLRW (Planck 2018)	4049	1625	2.49

Table 2. Covariance-weighted χ^2 statistics for the analytic model and the spatially flat FLRW model evaluated on the Pantheon+SH0ES supernova sample.

statistics. The resulting Hubble diagram and residuals are shown in Figure 3.

The Pantheon+SH0ES dataset Brout et al. (2022) provides observed distance moduli $\mu_{\text{obs}}(z)$ calibrated on an absolute scale via the SH0ES determination of the Type Ia supernova absolute magnitude Riess et al. (2022). This calibration is applied uniformly to both models.

Each model predicts $D_L(z)$, which is mapped to $\mu_{\text{th}}(z)$ using the definition of the distance modulus. We compare $\mu_{\text{th}}(z)$ to $\mu_{\text{obs}}(z)$ using the full Pantheon+ STAT+SYS covariance matrix.

We do not refit the FLRW model to the supernova sample, as this would convert the comparison into an in-sample descriptive fit rather than an out-of-sample predictive test. All models are therefore evaluated with parameters fixed independently of the supernovae used in the comparison. The analytic relation parameters are determined from galaxy kinematics and from Cepheid variable stars in the Pantheon+ dataset. This set of calibration records is then excluded from the evaluation, so the remaining supernovae provide an out-of-sample test of the predicted distance–redshift relation. The FLRW model is evaluated in a spatially flat form with parameters fixed to the Planck 2018 values, $\Omega_m = 0.315$, $\Omega_\Lambda = 1 - \Omega_m$, and $H_0 = 67.4 \text{ km s}^{-1} \text{ Mpc}^{-1}$ Planck Collaboration et al. (2020).

The resulting covariance-weighted chi-square statistics are summarized in Table 2.

The analytic relation yields a substantially lower covariance-weighted χ^2 and reduced χ^2 than the Planck 2018 FLRW model. The residuals as a function of redshift do not exhibit a clear systematic trend.

DATA AVAILABILITY

The data underlying this article are publicly available. The SPARC galaxy sample can be accessed at <http://astroweb.cwru.edu/SPARC/>, and the Pantheon+SH0ES Type Ia supernova dataset is available from the Pantheon+ data release at <https://github.com/PantheonPlusSH0ES/DataRelease> and the associated publications Brout et al. (2022); Riess et al. (2022). A computational notebook implementing the distance–redshift relation and observational analysis is available at <https://www.wolframcloud.com/obj/ed737c03-5baf-49f4-90e3-83b91b245c2a>. The notebook reproduces the results and figures presented in this work and is provided to enable independent verification of the calculations.

3 CONCLUSION

We test a phenomenological construction in which a single empirically determined acceleration scale links galaxy dynamics and cosmological distance measurements. The scale is fixed from galaxy kinematics, and a single additional parameter, calibrated on Cepheid variables, defines an analytic, closed-form distance–redshift relation.

When evaluated on the Pantheon+SH0ES supernova sample with

parameters fixed in advance, the resulting relation yields a substantially lower covariance-weighted χ^2 than a spatially flat Λ CDM model with Planck 2018 parameters, constituting an out-of-sample test of predictive performance.

The construction is directly falsifiable: with the acceleration scale and kinematic parameters fixed, it predicts a specific departure from Keplerian motion in bound systems such as the Solar System. This signal is absent from standard FLRW-based local dynamics without an additional local correction and is not a generic feature of MOND-like constructions. A robust non-detection would rule out the construction, while detection would provide a direct observational discriminator.

REFERENCES

- Brout D., Scolnic D., Popovic B., Riess A. G., et al., 2022, [Astrophysical Journal](#), 938, 110
- Guy J., et al., 2007, [Astronomy & Astrophysics](#), 466, 11
- McGaugh S. S., Schombert J. M., Bothun G. D., de Blok W. J. G., 2000, [Astrophysical Journal Letters](#), 533, L99
- McGaugh S. S., Lelli F., Schombert J. M., 2016, [Physical Review Letters](#), 117, 201101
- Milgrom M., 1983, [Astrophysical Journal](#), 270, 365
- Planck Collaboration Aghanim N., et al., 2020, [Astronomy & Astrophysics](#), 641, A6
- Riess A. G., Yuan W., Macri L. M., et al., 2022, [Astrophysical Journal Letters](#), 934, L7
- Scolnic D. M., et al., 2018, [Astrophysical Journal](#), 859, 101
- Tripp R., 1998, [Astronomy & Astrophysics](#), 331, 815